

## Application of a classical trajectory model to vibrational excitation in high-energy $H^+ + H_2$ collisions\*

W. Ronald Gentry

*Chemical Dynamics Laboratory, Chemistry Department, University of Minnesota, Minneapolis, Minnesota 55455*

Clayton F. Giese

*Tate Laboratory of Physics, School of Physics and Astronomy,  
University of Minnesota, Minneapolis, Minnesota 55455*

(Received 4 September 1974)

The method of distribution among quantum states of exact classical energy transfer (the DECENT model) for vibrational excitation in molecular collisions, in which three-dimensional classical trajectories are used to evaluate the quantum vibrational transition probabilities, is applied to  $H^+ + H_2$  and  $D^+ + H_2$  collisions at relative kinetic energies between 35 and 1000 eV. We compare the results with the experimental data of Herrero and Doering. Taking into account the scattering-angle discrimination in the experimental measurements, we find good agreement with experiment for the shapes of the energy dependence of the calculated total cross sections for individual final vibrational states and for the cross-section ratios. The absolute magnitudes of the calculated vibrational-excitation cross sections at high energies are about a factor of 2 larger than the experimental values, probably because of electronically nonadiabatic behavior ignored in the calculation, but a systematic discrepancy exists at lower energies which cannot be completely reconciled with the available experimental information.

### INTRODUCTION

There have recently been two extensive experimental studies of vibrational excitation in  $H^+ + H_2$  collisions in which individual  $H_2$  quantum vibrational transitions were resolved in the energy spectra of the scattered  $H^+$ . The relative differential cross sections for specific final vibrational states were measured in this laboratory for collisions of  $H^+$  with  $H_2$ , HD, and  $D_2$  at low relative kinetic energies (4–21 eV).<sup>1</sup> At high energies (80–1200 eV), the integral cross sections for excitation of resolved vibrational states were measured by Herrero and Doering for small-angle scattering of  $H^+$  and  $D^+$  from  $H_2$ .<sup>2</sup> Taken together these investigations provide perhaps the most extensive set of detailed microscopic data on state-resolved vibrational excitation in molecular collisions available for any one chemical system.<sup>3</sup> From an experimental point of view the  $H^+ + H_2$  system is an ideal one in which to study vibrational excitation because of the unusually large magnitude of the excitation cross sections and because of the large vibrational energy-level spacing of the  $H_2$  molecule. Happily, this system is also a convenient one for theoretical investigation. The Born-Oppenheimer ground-state potential energy has in fact already been calculated accurately for a large number of configurations in the range explored by the experiments.<sup>4</sup>

In a previous paper,<sup>5</sup> we reported a theoretical investigation of vibrational excitation in  $H^+ + H_2$

collisions in the low-energy regime. The calculations employed the DECENT model [distribution (among quantum states) of exact classical energy transfer], which takes advantage of the special correspondence between the classical and quantum-mechanical equations of motion for a forced harmonic oscillator. The probability distribution of final quantum vibrational states in the DECENT approximation is calculated from the exact classical vibrational energy acquired during the collision by an initially stationary oscillator. For each impact parameter and initial molecular orientation, the classical energy transfer was obtained by direct numerical integration of the classical equations of motion, using a potential-energy surface in the form of an accurate analytic fit to the available *ab initio* points for the ground electronic state of  $H^+ + H_2$ . The low-energy DECENT-model calculations yielded quantum transition probabilities in quantitative agreement with the experimental values (within the experimental uncertainty), and reproduced reasonably well the experimental differential cross sections, including the second classical rainbow associated with the potential-energy anisotropy. Here we apply the DECENT model to  $H^+ + H_2$  collisions in the high-energy regime of the Herrero and Doering experiments. In two respects, the DECENT model should be an even better approximation at higher energies. Certainly the use of a classical trajectory for the translational motion is more highly justified. Also, the prescription used in the DECENT model

to calculate the quantum transition probabilities from the classical energy transfer is exact only for a forcing potential which is linear in the vibrational coordinate. As the collision velocity is increased and the vibrational energy transfer becomes more impulsive, the excursion of the vibrational coordinate during the collision is decreased and therefore the effect of nonlinear terms in the driving potential should be reduced. Another approximation in the DECENT model, however, will break down at sufficiently high kinetic energies. Like almost every other theory of vibrational excitation in molecular collisions, the DECENT model assumes that the nuclear motion is determined by a Born-Oppenheimer potential-energy surface. For collision velocities within an order of magnitude of the molecular-electron velocities, this assumption becomes suspect, and such velocities are in fact reached in  $H^+ + H_2$  collisions at energies of a few hundred electron volts. At these energies the charge-transfer channel ( $H + H_2^+$ ), which corresponds at large separations to the lowest-energy excited electronic state of  $H_3^+$ , becomes important. Herrero and Doering measured only the vibrational excitation in the ground electronic state of the collision products and it is this data to which the calculations must be compared. It is of interest to find out how well those collisions at high energy which result in no electronic transition can be described in terms of the simple  $H^+ + H_2$  ground-state potential-energy surface.

A previous semiclassical investigation of vibrational excitation in high-energy  $H^+ + H_2$  collisions has been made by Ritchie,<sup>6</sup> who used a model potential-energy surface and different dynamical approximations than those employed here. We also compare our results to his.

#### PROCEDURE

The potential-energy function used and the method for calculating individual classical trajectories were exactly as described in our previous paper.<sup>5</sup> The potential-energy surface is one corresponding to the electron configuration of  $H^+ + H_2$  at all separations, and was obtained by a least-squares-fitting procedure, using as data primarily the points calculated by Csizmadia *et al.*<sup>4</sup> At large separations the potential was required to go over smoothly to a slightly modified<sup>5</sup> Hulbert-Hirschfelder potential function for  $H_2$  (Ref. 7) plus long-range terms arising from the charge-quadrupole and charge-induced dipole contributions. The classical equations of motion in Hamiltonian form were integrated in coordinates of the Cartesian components of  $\vec{R}$ , the location of the ion with respect to the  $H_2$  center of mass, and  $\vec{r}$ , the location

of one of the  $H_2$  nuclei with respect to the other. A three-speed Adams-Moulton routine was used for the numerical integration. The initial step size was set sufficiently small for each run to enforce the conservation of total energy to within 0.005 eV.<sup>8</sup>

Since detailed information on the angular distributions was not required for comparison with the high-energy experiments, the Monte Carlo interpolation procedure employed to calculate the low-energy differential cross sections was not followed in this study. Instead, a conventional Monte Carlo treatment was performed, with properly weighted random selection of the impact parameter (over the range  $0 \leq b \leq 7.0$  bohr) and the initial molecular-orientation angles for each trajectory. As required by the DECENT-model rationale, the molecule was initially given zero vibrational energy. Since the collision is essentially instantaneous compared to the rotational period of  $H_2$ , the initial rotational speed was also taken to be zero. The probability  $P_n$  of transition to the  $n$ th vibrational state was calculated for each trajectory from the final classical vibrational energy  $\mathcal{E}$  according to the prescription

$$P_n = \epsilon^n e^{-\epsilon} / n!, \quad (1)$$

where  $\epsilon = \mathcal{E} / \hbar\omega$ . The vibrational-energy-level spacing  $\hbar\omega$  was taken to be 0.516 eV, the energy of the  $n=0 \rightarrow n=1$  transition in  $H_2$ .

The total cross section for excitation to the  $n$ th vibrational state is therefore simply proportional to the average value of  $P_n$ ,

$$\sigma_n = 43.1 \bar{P}_n \text{ \AA}^2. \quad (2)$$

For each energy and isotopic variation, 1000 trajectories were calculated, yielding estimated average standard deviations of 3.7% for  $\sigma_1$ , 9.8% for  $\sigma_2$ , and 24% for  $\sigma_3$ .

#### RESULTS AND DISCUSSION

We calculated total cross sections for transitions to the first three vibrationally excited states of  $H_2$  at nine energies for collisions with  $H^+$  and at six energies for  $D^+$  collisions. The values obtained are given in Table I, which also includes the low-energy total cross sections obtained previously<sup>5</sup> for  $H^+ + H_2$ . In Figs. 1 and 2 we compare the calculated cross sections with the experimental values of Herrero and Doering. All kinetic energies plotted or tabulated in this paper refer to the center-of-mass (c.m.) coordinate system.

The calculated total cross sections for both  $H^+ + H_2$  and  $D^+ + H_2$  exceed the measured cross sections by more than a factor of 2 over the entire energy range studied. This is partly due to the fact that the experimental values plotted are not

the actual total cross sections, but rather the integral cross sections for vibrational-excitation collisions which scatter the projectile ion into the detector, which accepts only those ions contained within a narrow spatial and angular range around the unscattered beam. This quantity should accurately represent the total cross section at high collision energies, where there is negligible probability for scattering outside the detector acceptance band, but at low energies will be less than the true total cross section. A cross section corresponding precisely to the experimentally measured value could be calculated, but only if the transmission probability of the instrument is known as a function of both the spatial coordinates of the scattering event and the polar and azimuthal scattering angles. It is also necessary to know the primary-ion-beam velocity-vector distribution and three-dimensional flux density within the collision cell. The measured quantity is then the convolution of the differential scattering cross section with the primary-beam spatial- and velocity-vector distributions, multiplied at each point by the detector transmission function and integrated over the detector spatial and angular passbands. Unfortunately, the information required for this calculation is not available. We have, however,

TABLE I. Total vibrational-excitation cross sections for  $H^+ + H_2$  and  $D^+ + H_2$  collisions from the DECENT-model calculations.

Energy (eV)	$\sigma_1$ ( $\text{\AA}^2$ )	$\sigma_2$ ( $\text{\AA}^2$ )	$\sigma_3$ ( $\text{\AA}^2$ )
$H^+ + H_2$			
6	2.30	0.66	0.32
10	4.12	1.06	0.34
16	5.66	1.92	0.66
25	6.21	2.31	0.82
45	6.20	2.04	0.65
70	6.01	1.79	0.49
100	5.42	1.35	0.35
140	5.29	1.17	0.27
200	4.30	0.78	0.17
300	3.42	0.46	0.073
450	2.59	0.28	0.049
700	2.08	0.20	0.041
1000	1.55	0.12	0.023
$D^+ + H_2$			
35	5.95	2.02	0.66
60	6.19	2.07	0.68
100	6.03	1.83	0.52
200	4.94	1.07	0.24
350	3.98	0.66	0.14
600	2.85	0.32	0.047
1000	1.95	0.16	0.025

crudely mimicked the experimental angular discrimination in a second set of calculations by eliminating contributions to the average values of  $P_n$  in Eq. (2) from trajectories deflected beyond a laboratory scattering angle of  $1.9^\circ$ , the half-maximum acceptance angle quoted by Herrero and Doering. The tails shown on the points for the calculated total cross sections in Figs. 1 and 2 indicate the corresponding integral cross sections for scattering within the laboratory angle range  $0^\circ \leq \theta \leq 1.9^\circ$ . These deviate strongly from the total cross sections at energies below about 100 eV, where the classical inelastic rainbow angles for some molecular orientations begin to exceed  $\theta = 1.9^\circ$ , but they still lie considerably above the experimental values.

Another consideration which affects the comparison between theory and experiment is the importance of the charge-transfer channel giving  $H + H_2^+$

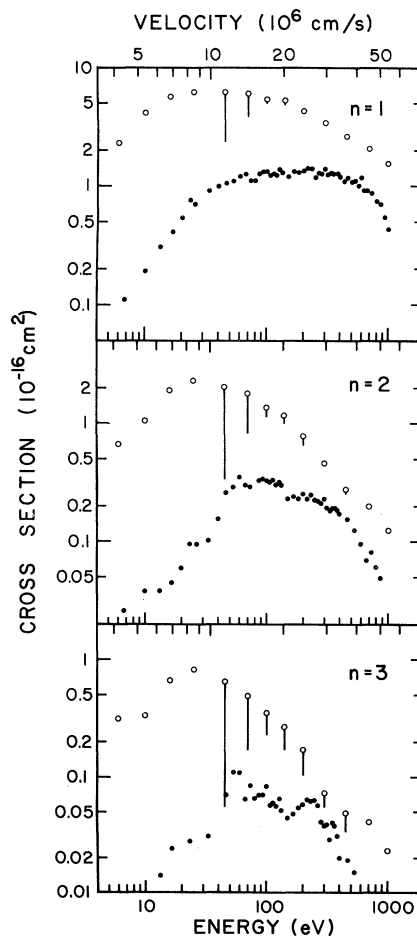


FIG. 1. Total cross sections for excitation of the first three vibrational states in  $H^+ + H_2$  collisions. Shaded points, data of Herrero and Doering; open circles, present calculated values. The bottoms of the tails on the calculated points indicate the cross sections obtained by excluding scattering beyond  $\theta = 1.9^\circ$  (lab).

as products. Since the experiment measures only vibrational excitation in the ground electronic state of  $H^+ + H_2$ , the effect of charge transfer is presumably to lower the vibrational excitation cross sections. Care must be exercised in such judgments, however, because the onset of charge transfer at high energies signals the breakdown of the Born-Oppenheimer approximation in which scattering on the ground-state surface is described. It is possible that the distortion of this surface through diabatic coupling will increase the probability for pure vibrational excitation. This seems unlikely in the  $H^+ + H_2$  system, since the vibrational excitation probabilities are already very large.

The charge-transfer cross section is a rapidly increasing function of energy in the range considered here. It rises from about  $0.4 \text{ \AA}^2$  at 100 eV to about  $7 \text{ \AA}^2$  at 1000 eV and reaches a broad maximum of about  $9 \text{ \AA}^2$  at 4000 eV.<sup>9</sup> Our theoretical treatment, which makes no provision for the charge-transfer channel, can therefore be expected to overestimate the vibrational excitation cross sections for ground-state products at energies above  $\sim 200$  eV. Below 100 eV, however, the effect of charge transfer should be small; therefore the discrepancy between theory and experiment remains unreconciled. It may, of course, be true that the DECENT-model calculation simply overestimates the vibrational transition probabilities by a factor of 2 or 3 in this energy range. In view of the good agreement obtained at energies of 6–16 eV between the measured and calculated transition probabilities at constant scattering angle, however, this would be very surprising.<sup>13</sup> Another possibility is that some source of discrimination against inelastically scattered protons in the experiment causes the measured cross sections to be too low. Some indication that this could be the case may be seen in the angular distributions reported by Herrero and Doering for inelastic  $H^+ + H_2$  scattering at a proton (laboratory) energy of 100 eV. The measured angular distributions of protons scattered with vibrational excitation of  $H_2$  to the  $n=1$  and  $n=2$  states were found to be nearly identical to that of the unscattered beam—a single peak with a full width at half-maximum (FWHM) angular width of  $\Delta\theta(\text{lab}) = 3.8^\circ$ .<sup>10</sup> This observation led Herrero and Doering to conclude that at 100 eV and higher laboratory energies, virtually all inelastically scattered ions were transmitted to the detector. The observed angular distribution does not, however, appear to be consistent with either the present calculations or with estimates based on the measured differential cross sections at lower energies. The angle of the rainbow maximum in the elastic differential

cross section for spherical-potential scattering is approximately inversely proportional to the collision energy. This relation was confirmed in the low-energy regime for both the inelastic and elastic differential cross sections for  $H^+ + H_2$ .<sup>1</sup> On this basis, the rainbow angle for vibrationally inelastic scattering of  $H^+$  from  $H_2$  at a c.m. energy of 70 eV should be at about  $\theta = 2.2^\circ$  (lab). Figure 3 shows the calculated angular distributions, which are consistent with this expectation. The FWHM angular spread for the  $n=1$  final state is  $5.4^\circ$  (lab). A crude estimate of the angular spread to be measured in the experiment is obtained by convoluting this distribution with the  $3.8^\circ$  FWHM instrumental-resolution function. This yields a distribution of approximately  $6.6^\circ$  FWHM, to be compared with the measured value of  $3.8^\circ$ . One possible explanation for this discrepancy is that the detector discriminates strongly against ions scattered through angles larger than the primary-beam divergence angle, in which case a serious error will be made

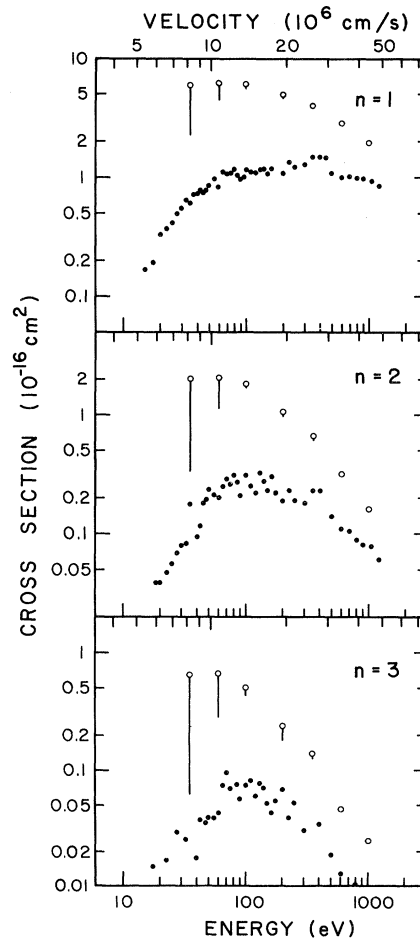


FIG. 2. Same as in Fig. 1, but for  $D^+ + H_2$  collisions.

in the determination of the total cross section. The issue can be resolved only with additional experimental information.

Aside from the absolute values of the vibrational excitation cross sections, the theoretical results are perfectly consistent with the major conclusions reached by Herrero and Doering, based on their experimental measurements. The calculated total cross sections have broad maxima in this energy range, with somewhat sharper peaks occurring at slightly lower energies for excitation to increasingly higher vibrational states. The theoretical maxima are found at lower energies than the experimental ones, as anticipated by Herrero and Doering, because in the experiments a greater fraction of the inelastically scattered  $H^+$  falls outside the range of detector acceptance angle at lower energies. Both the theoretical and experimental cross sections for  $D^+ + H_2$  collisions superimpose with those for  $H^+ + H_2$  when compared at the same collision velocity. The DECENT model provides a simple explanation for this observation. At high energies the translational motion is nearly uniform and rectilinear. For a specified impact parameter and initial velocity the ion-molecule separation  $R$  as a function of time is therefore the same for the two systems. The vibrational motion of the  $H_2$  molecule is caused primarily by the action of a stretching force  $F$  arising from the tem-

porary withdrawal of electron density from the molecular bond (bond dilution). Because  $R(t)$  is the same,  $F(t)$  and therefore the vibrational transition probabilities as well must also be the same in the two cases.

In Figs. 4 and 5, the DECENT-model calculations are compared with the experimental cross-section ratios, which do not depend on an absolute calibration of the detector efficiency. The agreement in this case is quantitative—well within the combined uncertainties of the experimental and calculated quantities. Again, the  $H^+ + H_2$  and  $D^+ + H_2$  results superimpose when compared at the same velocity.

The maximum in the vibrational-excitation cross sections occurs at the energy where there is, on the average, the most efficient match between the duration of the driving force  $F(t)$  and the molecular vibrational period. If the  $H_2$  vibrational-force constant were not altered by the interaction, the classical energy transfer would be determined by the Fourier component of  $F(t)$  at the vibrational frequency  $\omega$ ,<sup>11</sup>

$$\mathcal{G} = \frac{1}{2M} \left| \int_{-\infty}^{\infty} F(t) e^{-i\omega t} dt \right|^2.$$

The greatest energy transfer in this case would result if the stretching force acts over about one-

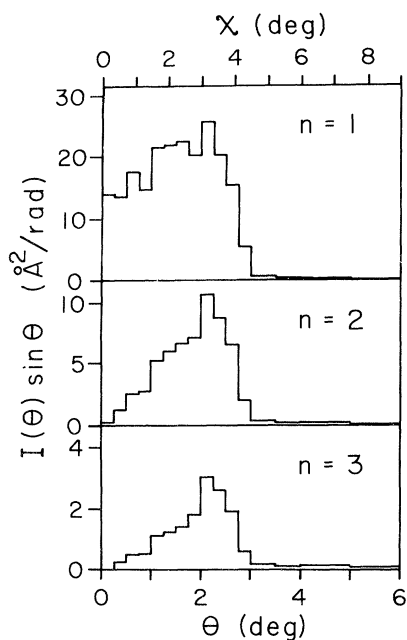


FIG. 3. Calculated differential cross sections for vibrationally inelastic scattering in 70-eV  $H^+ + H_2$  collisions (105-eV proton laboratory energy).  $\chi$  is the center-of-mass scattering angle and  $\theta$  is the laboratory scattering angle.

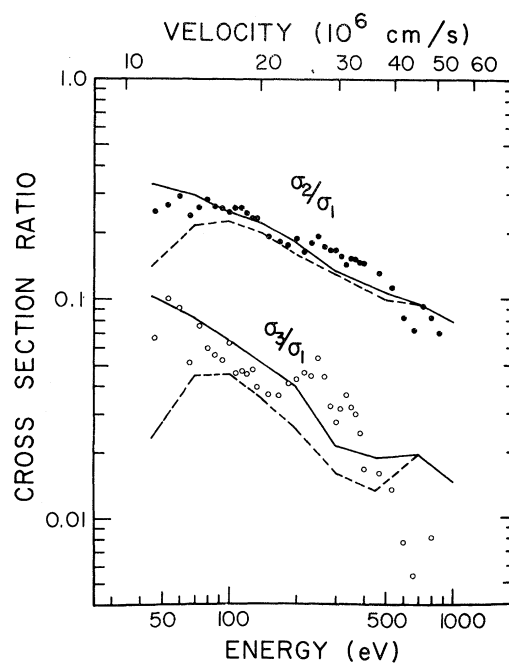


FIG. 4. Cross-section ratios for vibrationally inelastic scattering in  $H^+ + H_2$  collisions. Solid lines, calculated total-cross-section ratios; dashed lines, ratios obtained by excluding scattering beyond  $\theta = 1.9^\circ$  (lab). The points are from the data of Herrero and Doering.

half of a vibrational period. The actual situation is more complicated, since the molecular-force constant is a strong function of the configuration at small separations<sup>5</sup>; however, the same general concept still applies. At high energies, the forcing function becomes impulsive and the classical vibrational energy transfer for a given trajectory is simply inversely proportional to the kinetic energy  $E_0$ . Except for the breakdown of the Born-Oppenheimer approximation, the quantum transition probability for the  $0 \rightarrow n$  transition would therefore be proportional to  $E_0^{-n}$  in the high-energy limit. At low energies, where  $F(t)$  is longer in duration than half of a vibrational period, there is a great deal of cancellation in the effect of the driving force, resulting in a smaller cross section for vibrational excitation and extreme sensitivity of the result to the shape of the potential.<sup>12</sup>

In Fig. 6, we show histograms of the calculated vibrational transition probabilities as functions of impact parameter for  $H^+ + H_2$  collisions over the energy range 45–1000 eV. Just as at lower energies, there are two contributions to the total vibrational cross sections. The major contribution comes from large impact parameters where the interaction is of the “bond dilution” type. In addition, there is a contribution from small-impact-parameter collisions which explore the repulsive branch of the potential. Because the probability of an impact parameter  $b$  is proportional to  $b$ , the small- $b$  contribution is relatively minor. Several trends are evident from Fig. 6. The large-

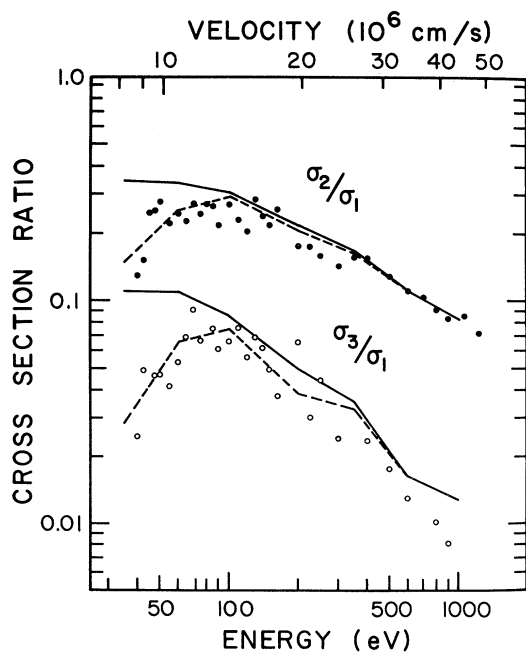


FIG. 5. Same as in Fig. 4, but for  $D^+ + H_2$  collisions.

$b$  excitation probabilities decrease with increasing energy, as do the cross sections. At lower energies, where the vibrational-excitation cross sections are increasing with energy, the opposite is true.<sup>5</sup> The higher the final vibrational state, the more sensitive is the transition probability to the average classical energy transfer. At large impact parameters, where  $\mathcal{E}$  is small compared to  $\hbar\omega$ ,  $P_n$  is approximately proportional to  $\mathcal{E}^n$ . This causes the cross section to peak more sharply in energy for excitation to a higher vibrational state. The relative importance of the small- $b$  contribution increases with kinetic energy and with the final vibrational quantum number. The transition probabilities calculated previously by Ritchie,<sup>6</sup> who treated the internal motion of the  $H_2$  molecule quantum mechanically rather than semi-classically, are qualitatively similar to those

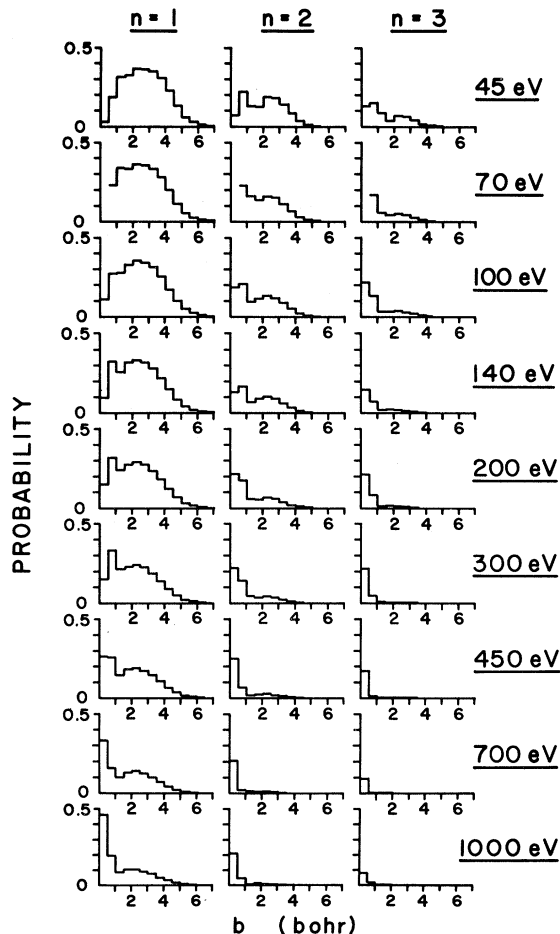


FIG. 6. Histograms of the average vibrational transition probabilities in  $H^+ + H_2$  collisions as functions of impact parameter and relative kinetic energy. These may be compared with the corresponding functions calculated with greater statistical accuracy at lower energies (Ref. 5).

shown in Fig. 6. The differences are attributable mainly to the different potential-energy surfaces employed. Ritchie assumed that the interaction primarily responsible for vibrational excitation is the polarization potential, which is much weaker than the real potential in the range  $2.5 < R < 5$  bohr. His calculated transition probabilities are therefore much smaller than ours within the corresponding range of impact parameter.

### CONCLUSIONS

The DECENT-model calculations, carried out with an accurate analytic representation of the Born-Oppenheimer ground-state potential surface, are consistent with the available experimental data on the shape of the energy dependence of the total cross section and the cross-section ratios for resolved vibrational excitation in  $H^+$ ,  $D^+ + H_2$  collisions at relative kinetic energies up to 1000

eV. The absolute magnitudes of the calculated cross sections are higher than the experimental values by a factor of 2-3, a discrepancy which cannot be attributed to the influence of the charge-transfer channel except at the highest energies in this range.

The calculations indicate that the primary mechanism for vibrational excitation at high energies is the same as that found at low energies. The withdrawal of electron density from the molecular bond (bond dilution) gives rise to a large stretching force acting between the  $H_2$  nuclei, even at rather large proton- $H_2$  separations. Small-impact-parameter collisions which explore the repulsive wall of the potential make only a small contribution to the total cross section for excitation to the first excited vibrational state of  $H_2$  at low energies, but this contribution grows relatively more important for higher final vibrational states and higher collision energies.

\*Research supported in part by the National Science Foundation, Grant No. 38759x, and by a grant from the University of Minnesota Computer Center.

<sup>1</sup>H. Udseth, C. F. Giese, and W. R. Gentry, *Phys. Rev. A* **8**, 2483 (1973); *J. Chem. Phys.* **54**, 3642 (1971).

<sup>2</sup>F. A. Herrero and J. P. Doering, *Phys. Rev. A* **5**, 702 (1972).

<sup>3</sup>A summary of other recent experimental work has been given by J. P. Doering, *Ber. Bunsenges. Phys. Chem.* **77**, 593 (1973).

<sup>4</sup>I. G. Csizmadia, R. E. Kari, J. C. Polanyi, A. C. Roach, and M. A. Robb, *J. Chem. Phys.* **52**, 6205 (1970); C. W. Bauschlicher, S. V. O'Neil, R. K. Preston, H. F. Schaefer III, and C. F. Bender, *J. Chem. Phys.* **59**, 1286 (1973); G. D. Carney and R. N. Porter, *J. Chem. Phys.* **60**, 4251 (1974).

<sup>5</sup>C. F. Giese and W. R. Gentry, *Phys. Rev. A* **10**, 2156 (1974).

<sup>6</sup>B. Ritchie, *Phys. Rev. A* **6**, 1902 (1972).

<sup>7</sup>H. M. Hulburt and J. O. Hirschfelder, *J. Chem. Phys.* **9**, 61 (1941).

<sup>8</sup>This criterion ensured that the vibrational energy trans-

fer for each collision was accurate to 0.001 eV. See Ref. 5.

<sup>9</sup>J. B. H. Stedeford and J. B. Hasted, *Proc. R. Soc. A* **227**, 466 (1955).

<sup>10</sup>The angular distributions measured previously by J. H. Moore and J. P. Doering [*Phys. Rev. Lett.* **23**, 564 (1969)] show the distributions of inelastically scattered  $H^+$  to be broader than the unscattered beam.

<sup>11</sup>L. D. Landau and E. M. Lifshitz, *Mechanics*, 2nd ed. (Pergamon, New York, 1969).

<sup>12</sup>A similar observation on the sensitivity of the vibrational-excitation probabilities for  $He + H_2$  to the potential was made by M. H. Alexander and E. V. Berand, *J. Chem. Phys.* **60**, 3950 (1974).

<sup>13</sup>F. S. Collins, R. K. Preston, and R. J. Cross, *Chem. Phys. Lett.* **25**, 608 (1974), have reported both a quasi-classical trajectory calculation and a semiclassical calculation based on time-dependent perturbation theory for 10-eV  $H^+ + H_2$ . Using approximate potential-energy surfaces, these authors obtained total vibrational-excitation cross sections considerably larger than our values.